A Multilayer Saint-Venant Model

Emmanuel Audusse

INRIA

A Multilayer Saint-Venant Model

Emmanuel Audusse

N° 5249

Juillet 2004

Thème NUM

R apport de recherche

A Multilayer Saint-Venant Model

Emmanuel Audusse *

Abstract: We introduce a new variant of the multilayer Saint-Venant system. The classical Saint-Venant system is a well-known approximation of the incompressible Navier-Stokes equations for shallow water flows with free moving boundary. Its efficiency, robustness and low computational cost make it very commonly used. Nevertheless its range of application is limited and it does not allow to access to the vertical profile of the horizontal velocity. Hence and thanks to a precise analysis of the shallow water assumption we propose here a new approximation of the Navier-Stokes equations which consists in a set of coupled Saint-Venant systems, extends the range of validity and gives a precise description of the vertical profile of the horizontal velocity while preserving the computational efficiency of the classical Saint-Venant system. We validate the model through some numerical examples.

Key-words: Free surface Navier-Stokes equations, shallow water assumption, hydrostatic approximation, Saint-Venant system, multilayer model, viscosity

* Projet BANG

Un modèle Saint-Venant multicouche

Résumé : Nous introduisons une nouvelle variante d'un système de Saint-Venant multicouche. Le système de Saint-Venant classique est, de par son efficacité et sa robustesse, souvent utilisé pour modéliser les écoulements incompressibles à surface libre en eaux peu profondes. Néanmoins son domaine d'application reste limité et il ne donne accés qu'à une vitesse moyenne de l'écoulement. Grâce à une analyse détailée de l'hypothèse eaux peu profondes, nous proposons une nouvelle approximation des équations de Navier-Stokes, qui consiste en une série de systèmes de Saint-Venant couplés. Cette approche multicouche permet d'étendre le domaine de validité du modèle et fournit une description précise du profil vertical de vitesse horizontale, tout en préservant la simplicité et l'efficacité de l'approche Saint-Venant classique. Une validation du modèle au travers de l'étude d'une rupture de barrage est proposée.

Mots-clés : Equations de Navier-Stokes à surface libre, eaux peu profondes, approximation hydrostatique, système de Saint-Venant, modèle multicouche, viscosité

1   Introduction

In this paper we are interested in modeling the so-called shallow water flows. It covers a very large range of applications in the domain of the geophysical flows - rivers, lakes, costal areas, oceans, atmosphere, avalanches... In order to provide a new modelization step between the complexity of the full Navier-Stokes equations for incompressible flows with free surface and the loss of generality of the classical Saint-Venant system, we introduce in this paper a new multilayer Saint-Venant type model which consists in a set of coupled Saint-Venant systems

$$\frac{\partial h_\alpha}{\partial t} + \frac{\partial h_\alpha U_\alpha}{\partial x} = 0, \tag{1.1}$$

$$\frac{\partial h_\alpha U_\alpha}{\partial t} + \frac{\partial}{\partial x}\left(h_\alpha U_\alpha^2 + g\frac{h_\alpha \sum_{\beta=1}^{M} h_\beta}{2}\right)$$

$$= \frac{g\left(\sum_{\beta=1}^{M} h_\beta\right)^2}{2}\frac{\partial}{\partial x}\frac{h_\alpha}{\sum_{\beta=1}^{M} h_\beta} + 2\mu\frac{U_{\alpha+1} - U_\alpha}{h_{\alpha+1} + h_\alpha} - 2\mu\frac{U_\alpha - U_{\alpha-1}}{h_\alpha + h_{\alpha-1}}. \tag{1.2}$$

where $(h_\alpha, h_\alpha U_\alpha)(t,x)$ is the vector of the conservative variables - water height and discharge, thus $U_\alpha(t,x)$ is the velocity - and where the subscript α is related to the considered layer - thus $\alpha \pm 1$ are related to the neighbouring layers, above and below. M is the total number of layers. μ denotes the viscosity coefficient.

The main interest of such a formulation is to access to the vertical profile of the horizontal velocity while preserving the computational efficiency of the Saint-Venant model. Furthermore the model verifies some stability properties - existence of an energy, positivity of the water heights - and some physical properties - agreement with the classical Saint-Venant solution for compatible initial conditions, preservation of stationary states. One of the goals of the present paper is also to extend these properties to numerical simulation.

The classical Saint-Venant system [28] is a well known approximation of the free surface Navier-Stokes equations for shallow water flows, which has been widely validated for various geophysical flows, such as rivers or coastal areas [20], or even ocean and atmosphere dynamic or avalanches flows [5] when completed with appropriate terms.
The derivation of the Saint-Venant system from the Navier-Stokes equations for shallow incompressible flows with a free moving boundary is now classical when the viscosity is neglected [30]. But this does not allow to justify that the right jumps - that appear in dam breaks or hydraulic jumps - are those obtained when using the momentum - and not the velocity - as the conservative variable. In [15], Gerbeau and Perthame propose a full derivation based on an asymptotic analysis of the dimensionless Navier-Stokes equations. In particular they study the influence of the viscous term and its relation with the friction term. Then the classical Saint-Venant system with a friction term turns out to be a zeroth order

approximation of the Navier-Stokes equations for incompressible flows with a free moving boundary under the shallow water assumption. They also derive a viscous Saint-Venant system through a first order investigation. In a recent work [13], Saleri and Ferrari extended this approach to the 2D case including a slowly varying topography and an atmospheric pressure term.

Direct free surface Navier-Stokes computations are possible [21] but are still expensive and require sophisticated algorithms. It is necessary to adapt a 3D mesh to the movement of the free surface and to the variation of the bottom topography in sedimentation cases. It requires also to deal with the incompressibility condition. The Saint-Venant computations are much more efficient since they deal with unvarying 2D meshes. But the background of this computational simplification is also the main limitation of the Saint-Venant approach: it uses only integrated quantities. The classical Saint-Venant system is related to a "motion by slice" approximation, *i.e.* the horizontal velocity does not depend upon the vertical coordinate. Therefore some information is lost and the practical range of validity of the system is sometimes very limited: it fails to reproduce the correct vertical profile of the horizontal velocity - and even the correct averaged horizontal velocity - when the friction on the bottom is not small enough, also it is not able to reproduce such phenomena as the recirculation due to the surface wind in a closed lake.
For these reasons, intermediate models have been further used. Most of them are *simplified Navier-Stokes models*. In [9, 14, 25], Quarteroni, Saleri *et al.* consider this set of approximations of the 3D Navier-Stokes equations and they derive different approximate models. In particular, in [14, 25], they work on the so-called hydrostatic approximation in a way that is a first step toward the Saint-Venant model since they consider the integrated continuity equation to rise the water height as an explicit variable. Nevertheless the background of the modelization is still the classical Navier-Stokes formalism, at least for the horizontal momentum equation: unknowns are velocities and the continuous problem is considered on a 3D domain. The explicitation of the 2D+1D form of the problem is performed in a second step through the choice of the vertical discretization: the domain is divided into several layers on which the same 2D finite element approximation is used to describe the horizontal velocity. The layers can be fixed horizontal strata as in [14, 25] or based on the so-called sigma transformation as in [21].

Our approach can be seen as a *augmented Saint-Venant model*, i.e. a discretization of the 3D Navier-Stokes equations where the vertical grid (h_α) is evolved "à la Saint-Venant" and some viscous effects are kept. In this it goes one step further in the analysis of [15] and as for the classical Saint-Venant system we exhibit an energy and we characterize some equilibrium states. As one can see, the set of Saint-Venant sytems (1.1)-(1.2), being 2D, is able to preserve computational efficiency. The conservative form of the equations on water heights (h_α) leads to extend finite volume schemes to (1.1)-(1.2). This motivates our choice of writing (1.2) as an usual conservative left hand side plus non conservative corrections - on the right hand side. Indeed the challenge here would be to perform an algorithm able to

keep (i) stability - $h_\alpha \geq 0$ and entropy inequality (ii) conservation of heights and total momentum $\sum h_\alpha u_\alpha$ when $\nu = 0$ (iii) the particular states $h_\alpha = h/M$, $u_\alpha = u$ gives a consistent approximation of the classical monolayer Saint-Venant system - when $\nu = 0$ (iv) the steady states of a lake at rest are preserved. Our work provides a first step in this direction and can be related to a work of Saleri and Lazzaroni [22] motivated by the same applications. But the approaches are quite different since [22] presents non conservative Saint-Venant systems discretized through a finite element framework. In [6, 7] Pares *et al.* present a bi-fluid shallow water problem and the system they consider presents also common parts with the two layers version of (1.1)-(1.2). As in [22] they consider a non conservative version and they exhibit that the system is no more hyperbolic when the densities of the fluids are too close. We prove in the paper that the left hand side of the system (1.1)-(1.2) is hyperbolic which is another motivation for our formulation.

The outline of the paper is as follows. In Section 2 we apply the shallow water scaling to the free surface Navier-Stokes equations and we present and analyse two hydrostatic models - as indicated in Figure 1.1. Then in Section 3 we derive the multilayer Saint-Venant model (1.1)-(1.2) and we discuss its essential properties. In Section 4 we establish the discrete version of the model using the finite volume framework. In Section 5 we present some numerical results and comparisons between the monolayer Saint-Venant and Navier-Stokes systems which validate the model. Finally in Section 6 we conclude and present some perspectives.
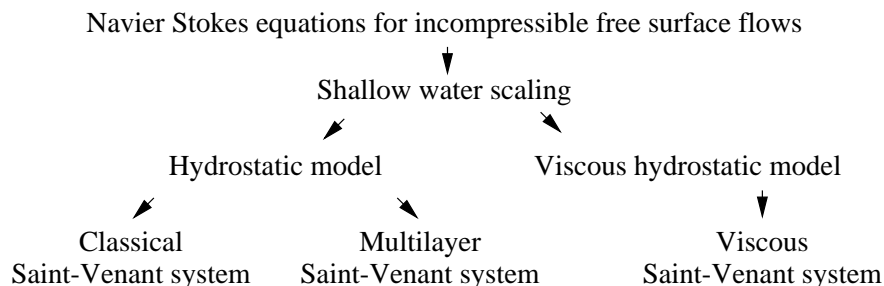
Navier Stokes equations for incompressible free surface flows

↓

Shallow water scaling

↙ ↘

Hydrostatic model   Viscous hydrostatic model

↙ ↘   ↓

Classical   Multilayer   Viscous
Saint-Venant system   Saint-Venant system   Saint-Venant system

Figure 1.1: From Navier-Stokes equations to Saint-Venant type models

2 Navier-Stokes equations and hydrostatic approximations

Following [15] we present here the first steps of the derivation of the Saint-Venant type models from the Navier-Stokes equations, *i.e.* the derivation of the simplified Navier-Stokes models - see Figure 1.1. We introduce a new focus on the question of the dissipation of the energy, whcich is an essential property of the Navier-Stokes equations. In particular it allows

us to discriminate an *energy compatible* form of the viscous hydrostatic model introduced in Subsection 2.1. Moreover we clearly distinguish the basic effects of the shallow water assumption - Subsection 2.1 - from the ones of further assumptions about viscosity and friction - Subsection 2.2.

We consider the classical free surface Navier-Stokes equations

$$\frac{\partial u}{\partial x} + \frac{\partial w}{\partial z} = 0, \tag{2.1}$$

$$\frac{\partial u}{\partial t} + \frac{\partial u^2}{\partial x} + \frac{\partial uw}{\partial z} + \frac{\partial p}{\partial x} = 2\mu\frac{\partial^2 u}{\partial x^2} + \mu\frac{\partial^2 u}{\partial z^2} + \mu\frac{\partial^2 w}{\partial x \, \partial z}, \tag{2.2}$$

$$\frac{\partial w}{\partial t} + \frac{\partial uw}{\partial x} + \frac{\partial w^2}{\partial z} + \frac{\partial p}{\partial z} = -g + \mu\frac{\partial^2 w}{\partial x^2} + \mu\frac{\partial^2 u}{\partial x \, \partial z} + 2\mu\frac{\partial^2 w}{\partial z^2}, \tag{2.3}$$

with

$$t > 0, \quad x \in \mathbb{R}, \quad 0 \leq z \leq h(t,x),$$

where $u(t,x,z)$ is the horizontal velocity, $w(t,x,z)$ is the vertical velocity, $p(t,x,z)$ the pressure and where $h(t,x)$ denotes the water height, g the gravity and μ the viscosity. Notice that for simplicity we consider the flat bottom case. In [13] Saleri and Ferrari extended the analysis of Gerbeau and Perthame [15] concerning the classical Saint-Venant model to a slowly varying bottom. The present work does not introduce new contribution on this particular topic and the same extension can be done for the multilayer model that we introduce in Section 3. Notice also that we assume that the free surface is a function of (x,t).

On the bottom we consider a no penetration condition and we estimate the friction through a coefficient κ and a Navier condition

$$w(t,x,0) = 0, \quad \mu\,\frac{\partial u}{\partial z}(t,x,0) = \kappa u(t,x,0). \tag{2.4}$$

On the free surface we consider a no stress condition

$$\mu\,\frac{\partial u}{\partial z} \;+\; p\,\frac{\partial h}{\partial x} \;-\; 2\mu\frac{\partial u}{\partial x}\,\frac{\partial h}{\partial x} \;+\; \mu\frac{\partial w}{\partial x} \;=\; 0 \quad \text{on} \quad z = h(t,x), \tag{2.5}$$

$$p \;-\; 2\mu\,\frac{\partial w}{\partial z} \;+\; \mu\frac{\partial u}{\partial z}\,\frac{\partial h}{\partial x} \;+\; \mu\frac{\partial w}{\partial x}\,\frac{\partial h}{\partial x} \;=\; 0 \quad \text{on} \quad z = h(t,x), \tag{2.6}$$

and the kinematic boundary condition

$$\frac{\partial h}{\partial t} + u(t,x,z = h(t,x))\frac{\partial h}{\partial x} - w(t,x,z = h(t,x)) = 0. \tag{2.7}$$

We recall that (2.1), (2.4) and (2.7) lead to the following mass equation

$$\frac{\partial h}{\partial t} + \frac{\partial}{\partial x}\int_0^h u\,dz = 0.$$

We recall also that a fundamental stability property is related to the fact that the Navier-Stokes equations admit an energy

$$e_{ns}(t,x,z) = e_c(t,x,z) + e_p(t,x,z) = \frac{u^2 + w^2}{2}(t,x,z) + gz.$$

and that the following equation holds

$$\frac{\partial}{\partial t} \int_0^h e_{ns} \, dz \; + \; \frac{\partial}{\partial x} \int_0^h \left(u(e_{ns} + p) - \mu \left(2u \frac{\partial u}{\partial x} + w \left(\frac{\partial u}{\partial z} + \frac{\partial w}{\partial x} \right) \right) \right) dz$$

$$= - \kappa u^2(t,x,0) \; - \; 2\mu \int_0^h \left[\left(\frac{\partial u}{\partial x} \right)^2 + \frac{1}{2} \left(\frac{\partial u}{\partial z} + \frac{\partial w}{\partial x} \right)^2 + \left(\frac{\partial w}{\partial z} \right)^2 \right] dz.$$

For further analysis of the full Navier-Stokes equations we refer to [24].

We are now interested in the shallow water flows. As usual we introduce two characteristic dimensions H and L in the vertical and horizontal directions respectively. The shallow water flows are then characterized by the fact that H is very small compared with L. Thus we can make the so-called shallow water assumption, i.e. we introduce a "small parameter" $\epsilon = \frac{H}{L}$. Then after rescaling we can write (2.1)-(2.3) as a dimensionless Navier-Stokes system

$$\frac{\partial u}{\partial x} + \frac{\partial w}{\partial z} \;=\; 0, \tag{2.8}$$

$$\frac{\partial u}{\partial t} + \frac{\partial u^2}{\partial x} + \frac{\partial uw}{\partial z} + \frac{\partial p}{\partial x} \;=\; 2\nu \frac{\partial^2 u}{\partial x^2} + \frac{\nu}{\epsilon^2} \frac{\partial^2 u}{\partial z^2} + \nu \frac{\partial^2 w}{\partial x \, \partial z}, \tag{2.9}$$

$$\epsilon^2 \left(\frac{\partial w}{\partial t} + \frac{\partial uw}{\partial x} + \frac{\partial w^2}{\partial z} \right) + \frac{\partial p}{\partial z} \;=\; -g + \epsilon^2 \nu \frac{\partial^2 w}{\partial x^2} + \nu \frac{\partial^2 u}{\partial x \, \partial z} + 2\nu \frac{\partial^2 w}{\partial z^2}. \tag{2.10}$$

Notice that $\nu = \mu/(UL)$ is the dimensionless form of the viscosity coefficient and that here and in all the dimensionless equations g does not denote the gravity but the Froude number $g/(UL)$.

The associated boundary conditions on the bottom (2.4) are rescaled as

$$w(t,x,0) = 0, \quad \frac{\nu}{\epsilon} \frac{\partial u}{\partial z}(t,x,0) = \gamma u(t,x,0), \tag{2.11}$$

where $\gamma = \kappa/U$ is the dimensionless form of the friction coefficient. The boundary conditions on the free surface (2.5)-(2.6) are rescaled as

$$\frac{\nu}{\epsilon^2} \frac{\partial u}{\partial z} + p \frac{\partial h}{\partial x} - 2\nu \frac{\partial u}{\partial x} \frac{\partial h}{\partial x} + \nu \frac{\partial w}{\partial x} \;=\; 0 \quad \text{on} \quad z = h(t,x), \tag{2.12}$$

$$p - 2\nu \frac{\partial w}{\partial z} + \nu \frac{\partial u}{\partial z} \frac{\partial h}{\partial x} + \epsilon^2 \nu \frac{\partial w}{\partial x} \frac{\partial h}{\partial x} \;=\; 0 \quad \text{on} \quad z = h(t,x). \tag{2.13}$$

The kinematic boundary condition (2.7) is unchanged.

2.1   A viscous hydrostatic model

We simplify the system (2.1)-(2.3) by retaining the zero and first order terms. We obtain a viscous hydrostatic model

$$\frac{\partial u}{\partial x} + \frac{\partial w}{\partial z} \;=\; 0, \tag{2.14}$$

$$\frac{\partial u}{\partial t} + \frac{\partial u^2}{\partial x} + \frac{\partial uw}{\partial z} + \frac{\partial p}{\partial x} \;=\; 2\nu\frac{\partial^2 u}{\partial x^2} + \frac{\nu}{\epsilon^2}\frac{\partial^2 u}{\partial z^2} + \nu\frac{\partial^2 w}{\partial x\,\partial z}, \tag{2.15}$$

$$\frac{\partial p}{\partial z} \;=\; -g + \nu\frac{\partial^2 u}{\partial x\,\partial z} + 2\nu\frac{\partial^2 w}{\partial z^2} + \epsilon^2\nu\,\frac{\partial^2 w}{\partial x^2}, \tag{2.16}$$

where

$$t > 0, \quad x \in \mathbb{R}, \quad 0 \le z \le h(t,x).$$

The associated boundary conditions are the same as the ones corresponding to the full dimensionless Navier-Stokes equations.

Remark 2.1 *Our motivation for keeping the second order term in the right hand side of the Navier-Stokes equations and in the free surface boundary conditions is that it is necessary for the energy dissipation as it is exhibited below. As it is an essential property of the Navier-Stokes equations we privilege this stability requirement to a strict first order approximation.*

Remark 2.2 *In (2.15)-(2.16) we have kept the symmetric form of the tensor - even though it can be simplified in Laplace terms - because of its natural relation to the boundary conditions (2.12)-(2.13).*

Now we check that the viscous hydrostatic approximation shares with the full Navier-Stokes equation on energy structure. We introduce the hydrostatic energy

$$e_h(t,x,z) = e_c(t,x,z) + e_p(t,x,z) = \frac{u^2}{2}(t,x,z) + gz. \tag{2.17}$$

Lemma 2.1 *The following energy equation holds for (2.14)-(2.16)*

$$\frac{\partial}{\partial t}\int_0^h e_h\,dz \;+\; \frac{\partial}{\partial x}\int_0^h \left(u(e_h + p) - \nu\left(2u\,\frac{\partial u}{\partial x} + w\,\frac{\partial u}{\partial z} + \epsilon^2 w\,\frac{\partial w}{\partial x}\right)\right)dz$$

$$= -\gamma u^2(t,x,0) - 2\nu\int_0^h\left[\left(\frac{\partial u}{\partial x}\right)^2 + \frac{1}{2}\left(\frac{1}{\epsilon}\,\frac{\partial u}{\partial z} + \epsilon\,\frac{\partial w}{\partial x}\right)^2 + \left(\frac{\partial w}{\partial z}\right)^2\right]dz.$$

Proof.   The proof uses classical computations. Following the purpose of Remark 2.1, let us notice the importance of the epsilon square term : it allows to include the term containing $\partial_z u\partial_x w$ in a square term and then to exhibit the decreasing of the energy.   □

The computational complexity and cost of this viscous hydrostatic model remain similar to the ones of the full Navier-Stokes equations. In particular we do not recover the classical hydrostatic approximation. One way to go further in the simplification is to introduce a scaling in the viscosity and friction coefficients. It seems to be in accordance with the physical background: indeed the viscosity coefficient can be related to the turbulent viscosity of the flow which is in particular related to the geometric datas and thus to the shallow water assumption. Nevertheless there is many ways to define this scaling: it is possible to consider anisotropic viscosity coefficients and also to introduce different powers of ϵ - see [4]. Here we shall suppose that we are in the following regime

$$\nu = \epsilon \nu_0, \qquad \text{and} \qquad \gamma = \epsilon \gamma_0. \tag{2.18}$$

2.2   A classical hydrostatic model

We consider the system (2.8)-(2.10) with the particular form of the viscosity and friction coefficients (2.18) and one retains only the zero order terms. We obtain the very classical hydrostatic model

$$\frac{\partial u}{\partial x} + \frac{\partial w}{\partial z} = 0, \tag{2.19}$$

$$\frac{\partial u}{\partial t} + \frac{\partial u^2}{\partial x} + \frac{\partial uw}{\partial z} + \frac{\partial p}{\partial x} = \frac{\nu_0}{\epsilon} \frac{\partial^2 u}{\partial z^2}, \tag{2.20}$$

$$\frac{\partial p}{\partial z} = -g, \tag{2.21}$$

where

$$t > 0, \quad x \in \mathbb{R}, \quad 0 \le z \le h(t,x).$$

After simplifying the terms of corresponding order, the boundary conditions (2.11)-(2.13) become

$$w(t,x,0) = 0, \tag{2.22}$$

$$\frac{\nu_0}{\epsilon} \frac{\partial u}{\partial z}(t,x,0) = \gamma_0 u(t,x,0), \quad \frac{\partial u}{\partial z}(t,x,h(t,x)) = 0, \tag{2.23}$$

$$p(t,x,h(t,x)) = 0. \tag{2.24}$$

The system is still associated with the kinematic boundary condition (2.7). Taking into account the pressure boundary condition on the free surface (2.24), (2.21) is equivalent to

$$p(t,x,z) = g(h(t,x) - z). \tag{2.25}$$

It is now possible to check that the hydrostatic approximation shares with the full Navier-Stokes equation on energy structure. Namely considering the hydrostatic energy (2.17),

Lemma 2.2 *The following equality holds for (2.19)-(2.24)*

$$\frac{\partial}{\partial t} \int_0^h e_h \, dz + \frac{\partial}{\partial x} \int_0^h u(e_h + p)dz \;=\; -\gamma_0 u^2(t,x,0) \;-\; \frac{\nu_0}{\epsilon} \int_0^h \left(\frac{\partial u}{\partial z}\right)^2 dz.$$

Proof. The proof uses on classical computations.   □

This hydrostatic model - or some variants with horizontal viscosity or other specific terms - is very used in geophysical flows studies. For further references see for example [4, 10, 19].

3   The Multilayer Saint-Venant System

We can now derive the Saint-Venant type models - see Figure 1.1. To do this we perform an asymptotic analysis of the hydrostatic models obtained in the previous section.
In [15] the authors present how to properly derive monolayer Saint-Venant models. Introducing an averaged velocity

$$U(t,x) = \frac{1}{h(t,x)} \int_0^h u(t,x,z)dz.$$

and departing respectively from the hydrostatic model (2.19)-(2.21) and from the viscous hydrostatic model (2.14)-(2.16) - under the hypothesis (2.18), they deduce the classical Saint-Venant system with friction

$$\frac{\partial h}{\partial t} + \frac{\partial hU}{\partial x} \;=\; 0, \tag{3.1}$$

$$\frac{\partial hU}{\partial t} + \frac{\partial}{\partial x}\left(hU^2 + \frac{gh^2}{2}\right) \;=\; -\kappa U. \tag{3.2}$$

and a viscous Saint-Venant system with friction

$$\frac{\partial h}{\partial t} + \frac{\partial hU}{\partial x} \;=\; 0, \tag{3.3}$$

$$\frac{\partial hU}{\partial t} + \frac{\partial}{\partial x}\left(hU^2 + \frac{gh^2}{2}\right) \;=\; -\frac{\kappa}{1 + \frac{\kappa h}{3\mu}}U + 4\mu\frac{\partial}{\partial x}\left(h\frac{\partial U}{\partial x}\right). \tag{3.4}$$

as formal asymptotic approximations in $O(\epsilon)$ - respectively $O(\epsilon^2)$ - of the Navier-Stokes equations. More details about these derivations can be found in [13, 15].
These two Saint-Venant models are associated with a dissipation of energy. Indeed introducing

$$hE = hE_c + hE_p = \frac{hU^2}{2} + \frac{gh^2}{2},$$

we establish for the classical Saint-Venant model (3.1)-(3.2)

$$\frac{\partial hE}{\partial t} + \frac{\partial}{\partial x}\left(U\left(hE + \frac{gh^2}{2}\right)\right) = -\kappa U^2,$$

and for the viscous ones (3.3)-(3.4)

$$\frac{\partial hE}{\partial t} + \frac{\partial}{\partial x}\left(U\left(hE + \frac{gh^2}{2}\right) - 4\mu\frac{\partial}{\partial x}\left(hU\frac{\partial U}{\partial x}\right)\right) = -\frac{\kappa}{1 + \frac{\kappa h}{3\mu}}U^2 - 4\mu h\left(\frac{\partial U}{\partial x}\right)^2.$$

Remark 3.1 *Notice that the classical Saint-Venant system (3.1)-(3.2) provides an exact solution to the hydrostatic system (2.19)-(2.21) when there is no friction on the bottom - i.e. $\gamma_0 = 0$. Indeed we can choose*

$$u(t,x,z) = U(t,x), \quad w(t,x,z) = -z\frac{\partial U}{\partial x}, \quad p(t,x,z) = g(h(t,x) - z),$$

where $(h,U)(t,x)$ is a solution of the classical Saint-Venant system (3.1)-(3.2). It is in general no more the case for the viscous models. Indeed a solution $(h_v, U_v)(t,x)$ of the viscous Saint-Venant system (3.3)-(3.4) - with no friction - provides a solution of the viscous hydrostatic system (2.14)-(2.16) if and only if it verifies also the following equality

$$4\frac{\partial}{\partial x}\left(h_v\frac{\partial U_v}{\partial x}\right) = 3h_v\frac{\partial^2 U_v}{\partial x^2}.$$

We now derive a more precise approximation. Especially we wish to keep some information on the vertical structure of the horizontal velocity as motivated in the introduction.

3.1   The Multilayer Saint-Venant model

We consider the hydrostatic model (2.19)-(2.21). We first introduce a discretization in the variable z - see Figure 3.1. Then for some $M \in \mathbb{N}$ we define M intermediate water heights $H_\alpha(t,x)$ such that

$$0 = H_0(t,x) \leq H_1(t,x) \leq H_2(t,x) \leq ... \leq H_{M-1}(t,x) \leq H_M(t,x) = h(t,x).$$

We characterize M layers through the definition of the indicator functions $\phi_\alpha(t,x,z)$

$$\forall \alpha \in \{1, M\} \quad \phi_\alpha(t,x,z) = \begin{cases} 1 & if \quad H_{\alpha-1}(t,x) \leq z \leq H_\alpha(t,x) \\ 0 & \text{otherwise,} \end{cases}$$

that are advected by the flow

$$\frac{\partial \phi_\alpha}{\partial t} + \frac{\partial \phi_\alpha u}{\partial x} + \frac{\partial \phi_\alpha w}{\partial z} = 0. \tag{3.5}$$
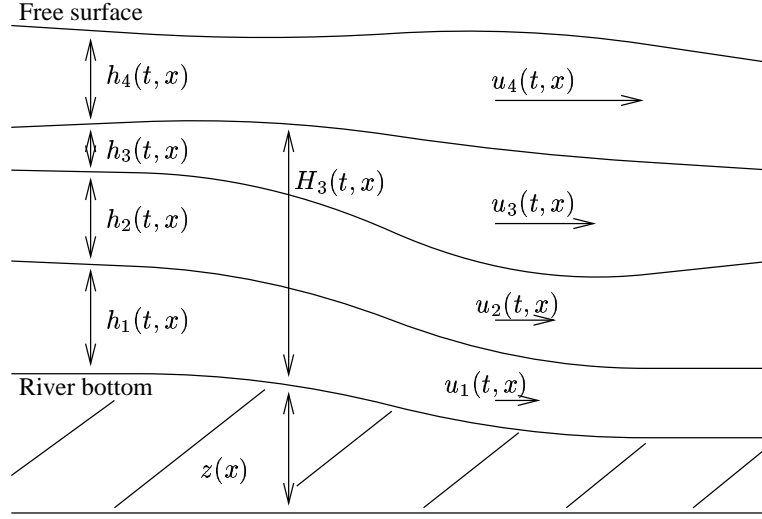
Figure 3.1: A multilayer approach

Then for each layer we define its water height $h_\alpha(t, x)$ by

$$\forall \alpha \in \{1, M\} \qquad h_\alpha(t, x) = H_\alpha(t, x) - H_{\alpha-1}(t, x),$$

and an averaged velocitiy $U_\alpha(t, x)$

$$\forall \alpha \in \{1, M\} \qquad U_\alpha(t, x) = \frac{1}{h_\alpha(t, x)} \int_{H_{\alpha-1}}^{H_\alpha} u(t, x, z) dz.$$

We claim that

Theorem 3.1 *The multilayer Saint-Venant system with friction defined by*

$$\frac{\partial h_1}{\partial t} + \frac{\partial h_1 U_1}{\partial x} = 0, \tag{3.6}$$

$$\frac{\partial h_1 U_1}{\partial t} + \frac{\partial}{\partial x}\left(h_1 U_1^2\right) + g h_1 \frac{\partial}{\partial x}\sum_{\beta=1}^{M} h_\beta = 2\mu \frac{U_2 - U_1}{h_2 + h_1} - \kappa U_1, \tag{3.7}$$

$$\frac{\partial h_\alpha}{\partial t} + \frac{\partial h_\alpha U_\alpha}{\partial x} = 0, \tag{3.8}$$

$$\frac{\partial h_\alpha U_\alpha}{\partial t} + \frac{\partial}{\partial x}\left(h_\alpha U_\alpha^2\right) + g h_\alpha \frac{\partial}{\partial x}\sum_{\beta=1}^{M} h_\beta = 2\mu \frac{U_{\alpha+1} - U_\alpha}{h_{\alpha+1} + h_\alpha} - 2\mu \frac{U_\alpha - U_{\alpha-1}}{h_\alpha + h_{\alpha-1}}, \tag{3.9}$$

$$for \quad \alpha = 2...M - 1$$

$$\frac{\partial h_M}{\partial t} + \frac{\partial h_M U_M}{\partial x} = 0, \tag{3.10}$$

$$\frac{\partial h_M U_M}{\partial t} + \frac{\partial}{\partial x}\left(h_M U_M^2\right) + g h_M \frac{\partial}{\partial x}\sum_{\beta=1}^{M} h_\beta = -2\mu\frac{U_M - U_{M-1}}{h_M + h_{M-1}}, \tag{3.11}$$

results from a formal asymptotic approximation in $O(\epsilon)$ coupled with a vertical discretization of the hydrostatic model and therefore of the Navier-Stokes equations.

Proof. We obtain by integration of (3.5) in the vertical direction M mass balance equations

$$\frac{\partial h_\alpha}{\partial t} + \frac{\partial}{\partial x}\int_{H_{\alpha-1}}^{H_\alpha} u\,dz = 0, \tag{3.12}$$

and M kinematic boundary conditions at the interfaces

$$\frac{\partial H_\alpha}{\partial t} + u(t,x,z=H_\alpha(t,x))\frac{\partial H_\alpha}{\partial x} - w(t,x,z=H_\alpha(t,x)) = 0. \tag{3.13}$$

Using the averaged velocities U_α we write the mass balance equations (3.12) in the Saint-Venant formalism

$$\frac{\partial h_\alpha}{\partial t} + \frac{\partial}{\partial x}h_\alpha U_\alpha = 0. \tag{3.14}$$

We now integrate on each layer the equation (2.20). The form of the hydrostatic pressure (2.25) leads to

$$\int_{H_{\alpha-1}}^{H_\alpha} \frac{\partial p}{\partial x}dz = \int_{H_{\alpha-1}}^{H_\alpha} g\frac{\partial h}{\partial x}dz = g\frac{\partial h}{\partial x}\int_{H_{\alpha-1}}^{H_\alpha} dz = g h_\alpha \frac{\partial h}{\partial x},$$

and thus we obtain - taking into account the kinematic boundary conditions (3.13) - M momentum equations

$$\frac{\partial}{\partial t}\int_{H_{\alpha-1}}^{H_\alpha} u\,dz + \frac{\partial}{\partial x}\int_{H_{\alpha-1}}^{H_\alpha} u^2\,dz + g h_\alpha \frac{\partial h}{\partial x} = \frac{\nu_0}{\epsilon}\frac{\partial u}{\partial z}(H_\alpha(t,x)) - \frac{\nu_0}{\epsilon}\frac{\partial u}{\partial z}(H_{\alpha-1}(t,x)). \tag{3.15}$$

Now equations (2.20) and (2.23) implie

$$\frac{\partial^2 u}{\partial z^2} = O(\epsilon), \qquad \frac{\partial u}{\partial z}|_{z=0} = O(\epsilon), \qquad \frac{\partial u}{\partial z}|_{z=h} = 0,$$

and therefore

$$u(t,x,z) = U(t,x) + O(\epsilon) \qquad \forall z \quad 0 \le z \le h(t,x), \tag{3.16}$$

what implies

$$\frac{1}{h_\alpha(t,x)}\int_{H_{\alpha-1}}^{H_\alpha} u^2(t,x,z)dz = U_\alpha^2(t,x) + O(\epsilon).$$

Hence we can write the momentum equations (3.15) in the Saint-Venant formalism

$$\frac{\partial}{\partial t} h_\alpha U_\alpha + \frac{\partial}{\partial x} h_\alpha U_\alpha^2 + g h_\alpha \frac{\partial h}{\partial x} = \frac{\nu_0}{\epsilon} \frac{\partial u}{\partial z}(H_\alpha(t,x)) - \frac{\nu_0}{\epsilon} \frac{\partial u}{\partial z}(H_{\alpha-1}(t,x)) + O(\epsilon). \qquad (3.17)$$

We drop the $O(\epsilon)$ and multiply (3.14) and (3.17) by HU^2/L in order to recover the variables with dimension. Finally we apply a finite difference method in the vertical direction to the right hand side of the momentum equations when it is concerned with an interface. $\square$

3.2 Properties of the Multilayer Saint-Venant System

The multilayer Saint-Venant systems presents two fundamental stability properties.

Proposition 3.1 *The multilayer Saint-Venant system (3.23)-(3.28) preserves the positivity of the water height in each layer. It is also associated with an energy inequality. Namely denoting $h = \sum_{\beta=1}^{M} h_\beta$ and introducing the energy*

$$E = \sum E_\alpha = \sum \left(\frac{h_\alpha U_\alpha^2}{2h} + \frac{g h_\alpha}{2} \right),$$

we establish the following equality

$$\frac{\partial}{\partial t} h E + \frac{\partial}{\partial x} \left(h \sum U_\alpha E_\alpha + h \sum U_\alpha \frac{g h_\alpha}{2} \right) = -\kappa U_1^2 - 2\mu \sum_2^M \frac{(u_\alpha - U_{\alpha-1})^2}{h_\alpha + h_{\alpha-1}}.$$

Proof. The development of the proof is very classical since it mimicks what is done for the classical Saint-Venant system. The new dissipative term in the energy equation is due to the presence of the same viscous friction term at the interface $\alpha - 1/2$ in the momentum equations for the layers α and $\alpha - 1$. $\square$

The multilayer Saint-Venant systems ensures also some relations with the classical Saint-Venant system

Proposition 3.2 *The multilayer Saint-Venant system (3.23)-(3.28) preserves the so-called lake at rest equilibrium*

$$\sum h_\alpha(0,x) = H, \qquad U_\alpha(0,x) = 0 \quad \forall \alpha = 1...M \qquad (3.18)$$

Also when there is no friction on the bottom the classical Saint-Venant system (3.1)-(3.2) provides a solution for the multilayer case. Indeed if we choose the initial conditions $U_\alpha(t = 0,x) = U_0(x)$ and $h_\alpha(t = 0,x) = c_\alpha H_0(x)$ (such that $\sum c_\alpha = 1$), a multilayer solution is given by

$$\forall \alpha = 1...M \qquad \left\{ \begin{array}{l} h_\alpha(t,x) = c_\alpha h(t,x), \\ U_\alpha(t,x) = U(t,x), \end{array} \right.$$

where $(h,U)(t,x)$ is a solution of the classical Saint-Venant system with initial values $(H_0, U_0)(t,x)$.

Proof. Proofs are obvious. Notice that the preservation of some steady states is a fundamental specific property of the Saint-Venant type models [3, 18]. The second point is is in agreement with Remark 3.1 since the multilayer system is an intermediate model between the hydrostatic system and the classical Saint-Venant system. □

3.3 Non conservativity and non hyperbolicity of the Multilayer Saint-Venant System

The multilayer Saint-Venant system (3.6)-(3.11) has two main drawbacks. First as opposed to the monolayer Saint-Venant models the pressure terms are not in a conservative form and thus their definition is not obvious when shocks occur. Nevertheless many works have been devoted to this question and some recent works propose numerical ways to choose a "right" solution - see [11] or [8] in the context of the Saint-Venant computations.

The second point is much more problematic. For the simplicity of the purpose let us consider the two layers version of the system (3.6)-(3.11). Following [6] we write the two layers system under the compact form

$$\frac{\partial X}{\partial t} + A(X)\frac{\partial X}{\partial x} = S(X), \tag{3.19}$$

where

$$X = \begin{pmatrix} h_1 \\ h_1 U_1 \\ h_2 \\ h_2 U_2 \end{pmatrix}, \qquad S(X) = \begin{pmatrix} 0 \\ 2\mu\dfrac{U_2 - U_1}{h_2 + h_1} - \kappa U_1 \\ 0 \\ 2\mu\dfrac{U_1 - U_2}{h_2 + h_1} \end{pmatrix},$$

$$A(X) = \begin{bmatrix} 0 & 1 & 0 & 0 \\ -U_1^2 + gh_1 & 2U_1 & gh_1 & 0 \\ 0 & 0 & 0 & 1 \\ gh_2 & 0 & -U_2^2 + gh_2 & 2U_2 \end{bmatrix}.$$

As the vertical profile of the velocity is given by the relation (3.16) we have

$$U_\alpha(t,x) = U(t,x) + O(\epsilon) \qquad \forall \alpha = 1, 2. \tag{3.20}$$

Proposition 3.3 *Under the assumption (3.20) the non conservative two layers Saint-Venant system (3.19) is not hyperbolic. Moreover when $U_1(t,x) \neq U_2(t,x)$ the eigenvalues of the matrix $A(X)$ have a non vanishing imaginary part.*

Proof. The eigenvalues of the matrix $A(X)$ are solutions of

$$\left(\lambda^2 - 2U_1\lambda + U_1^2 - gh_1\right)\left(\lambda^2 - 2U_2\lambda + U_2^2 - gh_2\right) = g^2 h_1 h_2.$$

Therefore under the assumption (3.20) first order approximations in $U_1 - U_2$ of the eigenvalues are

$$\lambda_{ext}^{\pm} = U_m \pm \sqrt{g(h_1 + h_2)}, \tag{3.21}$$

$$\lambda_{int}^{\pm} = U_c \pm i \frac{U_1 - U_2}{2} \sqrt{1 - \left(\frac{h_1 - h_2}{h_1 + h_2} \right)^2}, \tag{3.22}$$

where

$$U_m = \frac{h_1 U_1 + h_2 U_2}{h_1 + h_2}, \qquad U_c = \frac{h_1 U_2 + h_2 U_1}{h_1 + h_2}.$$

Notice that in the case $U_1 = U_2 = U$ the eigenvalues become real but the system is still not hyperbolic since U is a double eigenvalue associated with a one dimensional eigenspace. □

The eigenvalues $\lambda_{int}^{\pm}$ characterize the baroclinic part of the flow and are related to the celerity of a signal at the interface between the two layers [6, 16]. Their imaginary parts are related to the existence of instabilities at the interface which lead to a mixing between the two layers. Hence it is natural that the baroclinic eigenvalues of the multilayer system have a non vanishing imaginary part since the hypothesis (3.5) about the immiscibility of the layers is not linked to the physical background. But it follows also that the precise value of $\lambda_{int}^{\pm}$ is not relevant since we are not interested in the evolution of these "virtual" internal interfaces.

The two other eigenvalues $\lambda_{ext}^{\pm}$ characterize the barotropic part of the flow and are related to the celerity of a signal at the free surface. Therefore the multilayer Saint-Venant model is in agreement with the classical results about the monolayer Saint-Venant models for which the eigenvalues - and thus the celerities of a signal at the free surface - are $U \pm \sqrt{gh}$. Since these celerities are well-known to be in good accordance with the experiences, the agreement between the two models and thus the value of $\lambda_{ext}^{\pm}$ is an essential property of the multilayer system.

3.4   Conservative Form of the Multilayer Saint-Venant Model

To overcome the difficulties due to these non conservative structure and non hyperbolic nature of the multilayer Saint-Venant system (3.6)-(3.11) and therefore to avoid apparition of instabilities in the numerical simulations [6] we propose to consider a slightly different system

$$\frac{\partial h_1}{\partial t} + \frac{\partial h_1 U_1}{\partial x} = 0, \tag{3.23}$$

$$\frac{\partial h_1 U_1}{\partial t} + \frac{\partial}{\partial x} \left(h_1 U_1^2 + g \frac{h_1 \left(\sum_{\beta=1}^{M} h_\beta \right)}{2} \right)$$

$$= \frac{g \left(\sum_{\beta=1}^{M} h_\beta \right)^2}{2} \frac{\partial}{\partial x} \left(\frac{h_1}{\sum_{\beta=1}^{M} h_\beta} \right) + 2\mu \frac{U_2 - U_1}{h_2 + h_1} - \kappa U_1, \tag{3.24}$$

$$\frac{\partial h_\alpha}{\partial t} + \frac{\partial h_\alpha U_\alpha}{\partial x} = 0, \tag{3.25}$$

$$\frac{\partial h_\alpha U_\alpha}{\partial t} + \frac{\partial}{\partial x} \left(h_\alpha U_\alpha^2 + g \frac{h_\alpha \left(\sum_{\beta=1}^{M} h_\beta \right)}{2} \right)$$

$$= \frac{g \left(\sum_{\beta=1}^{M} h_\beta \right)^2}{2} \frac{\partial}{\partial x} \left(\frac{h_\alpha}{\sum_{\beta=1}^{M} h_\beta} \right) + 2\mu \left(\frac{U_{\alpha+1} - U_\alpha}{h_{\alpha+1} + h_\alpha} - \frac{U_\alpha - U_{\alpha-1}}{h_\alpha + h_{\alpha-1}} \right) \tag{3.26}$$

$$for \quad \alpha = 2...M - 1,$$

$$\frac{\partial h_M}{\partial t} + \frac{\partial h_M U_M}{\partial x} = 0, \tag{3.27}$$

$$\frac{\partial h_M U_M}{\partial t} + \frac{\partial}{\partial x} \left(h_M U_M^2 + g \frac{h_M \left(\sum_{\beta=1}^{M} h_\beta \right)}{2} \right)$$

$$= \frac{g \left(\sum_{\beta=1}^{M} h_\beta \right)^2}{2} \frac{\partial}{\partial x} \left(\frac{h_M}{\sum_{\beta=1}^{M} h_\beta} \right) - 2\mu \frac{U_M - U_{M-1}}{h_M + h_{M-1}}. \tag{3.28}$$

Proposition 3.4 *Under the assumption (3.16) this new set-up of the same system has the following properties*
(P1) The system obtained by replacing the right-hand side by zero is hyperbolic.
(P2) The barotropic eigenvalues $\lambda_{ext}^{\pm}$ (3.21) are still first order approximations in $U_1 - U_2$ of two of its eigenvalues.
(P3) For suitable initial water height data, the non conservative terms in the right hand side are "small" - they vanish in the Saint-Venant approximation $h_\alpha = h/M$, $U_\alpha = U$.
(P4) The sum on all the layers of the equations that describe the evolution of the water height and of the discharge in each layer is a first order approximation of the classical Saint-Venant system - left and right hand side considered separately.

Proof. As for the non conservative model we consider for simplicity the two layers case. Hence the eigenvalues of the matrix on the left hand side are solutions of

$$\left(\lambda^2 - 2U_1 \lambda + U_1^2 - gh_1 - \frac{gh_2}{2} \right) \left(\lambda^2 - 2U_2 \lambda + U_2^2 - gh_2 - \frac{gh_1}{2} \right) = \frac{g^2 h_1 h_2}{4}.$$

Therefore under the assumption (3.20) first order approximations of the eigenvalues are

$$\lambda_{ext}^{\pm} = U_m \pm \sqrt{g(h_1 + h_2)},$$

$$\lambda_{int}^{\pm} = U_c \pm \sqrt{\frac{g(h_1 + h_2)}{2}},$$

where

$$U_m = \frac{h_1 U_1 + h_2 U_2}{h_1 + h_2}, \qquad U_c = \frac{h_1 U_2 + h_2 U_1}{h_1 + h_2}.$$

Properties (P1) and (P2) follow immediately. Properties (P3) and (P4) are consequences of obvious computations - notice that "suitable initial water height data" means that the initial non conservative pressure source term is small. The second part of (P3) means that in the zero friction case, and for suitable initial data, the non conservative pressure source term P and the viscous source term V vanish for each time.

$$P = \frac{g}{2} \left(\sum_{\beta=1}^{M} h_\beta \right)^2 \partial_x \left(\frac{h}{\sum_{\beta=1}^{M} h_\beta} \right), \quad V = 2\mu \left[\frac{(U_{\alpha+1} - U_\alpha)}{(h_{\alpha+1} + h_\alpha)} - \frac{(U_\alpha - U_{\alpha-1})}{(h_\alpha + h_{\alpha-1})} \right]$$

A consequence of (P4) is that the free surface and the total discharge of the multilayer system are first order approximation of the classical Saint-Venant results, plus corrections due to the more sophisticated vertical profile of the flow velocity. □

Remark 3.2 *Outside from the dry areas the conservative part of the two layers system is strictly hyperbolic. Nevertheless it is no more the case when we consider a multilayer system with three or more layers since the multiplicity of the eigenvalues $\lambda_{int}^{\pm}$ is equal to the number of interfaces - at least for the case $U_\alpha = U$. The system is still hyperbolic since the dimensions of the associated eigenspaces are also equal to the number of interfaces - see Serre [29], Dafermos [12] for precise definitions.*

Remark 3.3 *The most intuitive form for a conservative multilayer model is the one which mimicks exactly the flux of the classical Saint-Venant system (3.1)-(3.2) by introducing $\partial_x g h_\alpha^2$ as conservative pressure term. The non conservative part is then $g h_\alpha \partial_x \sum_{\beta \neq \alpha} h_\beta$ and can be interpreted as a topographic source term. The conservative part is hyperbolic since the eigenvalues are - for each layer - deduced from those of the classical Saint-Venant system. Also the strict analogy with the classical Saint-Venant system seems to be convenient for computational use. Nevertheless this method is in fact defective since it does not respect any of the three properties (P2)-(P4) and especially the eigenvalues of the hyperbolic system of the left hand side are far from the barotropic eigenvalues $\lambda_{ext}^{\pm}$ (3.21).*

Remark 3.4 *Both set-ups of the multilayer model preserve the lake at rest steady state. But if we have in mind the numerical treatment of this equilibrium state it is important to notice that, if for the non-conservative model and at the lake at rest equilibrium state both fluxes*

*and source terms vanish, on the contratry, for the conservative model and always at the lake
at rest equilibrium state fluxes and source terms are equal but different from zero. It follows
that the situation for the conservative case is very similar to the preservation of the classical
(monolayer) Saint-Venant lake at rest equilibrium in the presence of a non zero topographic
term. And it is well known that the preservation of this equilibrium at the discrete level is
far from being obvious [3, 18].*

4   The discrete multilayer scheme

We now present the discrete version of the conservative multilayer Saint-Venant system
(3.23)-(3.28). The conservative multilayer Saint-Venant system (3.23)-(3.28) presents some
new terms when compared with the classical Saint-Venant system (3.1)-(3.2) - in the source
terms and even in the conservative part. Several strategies are possible and for instance
Pares et al. [6] prefer to consider the full system and built a specific solver for the two layers
case. Since here we wish to treat as many layers as possible we follow another strategy
that can be seen as a modified layer-by-layer approach - with respect to the terminology
introduced in [6]. Indeed we consider the multilayer system as M coupled modified Saint-
Venant systems and we choose to adapt an existing Saint-Venant finite volume solver to the
multilayer case - for a general introduction to the finite volume methods refer to [17, 23].
Especially the discretization technics have to preserve the properties of the continuous mul-
tilayer model stated in the Propositions 3.1 and 3.2.

To approximate the solution $(h_\alpha(t,x), U_\alpha(t,x)), \alpha = 1..M$ of the multi-layer Saint-Venant
system by discrete values $(h_{\alpha j}^n, U_{\alpha j}^n), \alpha = 1..M, j \in \mathbb{Z}, n \in \mathbb{N}$ we introduce as usual a space-
time discretization based on a grid of points $x_{j+1/2}$ with space steps $\Delta x_j = x_{j+1/2} - x_{j-1/2}$
and on a grid of points t^n defined by $t^n = \sum_{k \leq n} \Delta t^k$ where the time steps Δt^k will be
precised later through a CFL condition. Then we use the finite volume framework.
We choose to include explicitely the pressure source term in the finite volume solver. This
follows usual ideas for bottom topographies - refer to [1]. The viscosity source term can be
interpreted as a friction term between the layer we are considering and the two neighbouring
layers. As usual we treat this friction term implicitly. This leads to solve a linear system.
For the simplicity of the purpose we now divide the computation in two steps : explicit com-
putation of the fluxes taking into account the pressure source term and implicit computation
of the friction source terms.

4.1   The finite volume solver

To perform the explicit step we use a finite volume kinetic scheme. The general form of a
finite volume method is

$$X_{\alpha j}^{n+\frac{1}{2}} - X_{\alpha j}^n + \sigma_j^n [F_{\alpha,j+\frac{1}{2}}^n - F_{\alpha,j-\frac{1}{2}}^n] - \Delta t^n\, S_{\alpha j}^n = 0,$$

where $X_{\alpha j}^n = \left(h_{\alpha j}^n, q_{\alpha j}^n = h_{\alpha j}^n U_{\alpha j}^n \right)$ is the vector of the unknowns, $\sigma_j^n = \Delta t^n / \Delta x_j$ is the ratio between space and time steps, and where the discrete flux $F_{\alpha,j+\frac{1}{2}}^n$ is an approximation of the exact flux estimated at point $x_{j+\frac{1}{2}}$.

The kinetic scheme is a particular way to construct the numerical flux. For the case of the Saint-Venant system it presents a very good compromise between stability and accuracy. Thanks to a microscopic interpretation of the equations it allows to construct macroscopic schemes that preserve some essential properties of the continuous model: positivity of the water height, entropy inequality, ability to treat vacuum areas... We refer to [26] for a general survey of the kinetic theory and to [2, 27] for further details about kinetic schemes for the Saint-Venant system.

The multilayer conservative pressure term does not fit exactly in the usual frame work of the Saint-Venant type models. Thus it is not obvious that all the finite volume schemes that have been developped to solve the classical Saint-Venant system can be extend to the multilayer case. We claim that the extension of the kinetic scheme to the multilayer case is very natural. It is another argument for its choice. In fact the only difference with the classical case arises in the definition of the Gibbs equilibrium that appears in the microscopic interpretation of the Saint-Venant system. Indeed the modified Gibbs equilibrium involves at the same time the water height of the layer and the total water height of the flow. More precisely and with respect to the notations in [2] the Gibbs equilibrium for the layer α is now

$$M_\alpha(t,x,\xi) = \frac{h_\alpha(t,x)}{c(t,x)} \chi\left(\frac{\xi - U_\alpha(t,x)}{c(t,x)}\right),$$

where

$$c(t,x) = \sqrt{\frac{g\sum_{\beta=1}^M h_\beta(t,x)}{2}}.$$

The new non conservative pressure source term is discretized through a minmod limiter to ensure the robustness of the scheme

$$S_{\alpha j}^n = \left(\begin{array}{c} 0 \\ \frac{g\left(\sum_{\beta=1}^M h_{\beta j}^n\right)^2}{2} \text{minmod}\left(\frac{h_{\alpha,j+1}^n}{\sum_{\beta=1}^M h_{\beta,j+1}^n} - \frac{h_{\alpha j}^n}{\sum_{\beta=1}^M h_{\beta j}^n}, \frac{h_{\alpha j}^n}{\sum_{\beta=1}^M h_{\beta j}^n} - \frac{h_{\alpha,j-1}^n}{\sum_{\beta=1}^M h_{\beta,j-1}^n} \right) \end{array} \right). \tag{4.1}$$

4.2   The implicit computation

This implicit step does not affect the discrete water heights. Therefore

$$h_{\alpha j}^{n+1} = h_{\alpha j}^{n+\frac{1}{2}}. \tag{4.2}$$

The computation of the new velocities $U_{\alpha j}^{n+1}$ leads to the computation of a tridiagonal $M \times M$ linear system

$$
\begin{bmatrix}
a_{1j} & b_{1j} & 0 & \cdots & 0 \\
c_{2j} & \ddots & \ddots & \ddots & \vdots \\
0 & \ddots & \ddots & \ddots & 0 \\
\vdots & \ddots & \ddots & \ddots & b_{M-1,j} \\
0 & \cdots & 0 & c_{Mj} & a_{Mj}
\end{bmatrix}
\begin{bmatrix}
U_{1j}^{n+1} \\
\vdots \\
\vdots \\
\vdots \\
U_{Mj}^{n+1}
\end{bmatrix}
=
\begin{bmatrix}
q_{1j}^{n+\frac{1}{2}} \\
\vdots \\
\vdots \\
\vdots \\
q_{Mj}^{n+\frac{1}{2}}
\end{bmatrix},
\qquad (4.3)
$$

where

$$
a_{1j} = h_{1j}^{n+1} + \frac{2\mu \Delta t^n}{h_{1j}^{n+1} + h_{2j}^{n+1}} + \kappa \Delta t^n,
$$

$$
a_{\alpha j} = h_{\alpha j}^{n+1} + 2\mu \Delta t^n \left(\frac{1}{h_{\alpha j}^{n+1} + h_{\alpha+1,j}^{n+1}} + \frac{1}{h_{\alpha j}^{n+1} + h_{\alpha-1,j}^{n+1}} \right) \qquad \alpha = 2...M-1,
$$

$$
a_{Mj} = h_{Mj}^{n+1} + \frac{2\mu \Delta t^n}{h_{Mj}^{n+1} + h_{M-1,j}^{n+1}}, \qquad (4.4)
$$

$$
b_{\alpha j} = -\frac{2\mu \Delta t^n}{h_{\alpha j}^{n+1} + h_{\alpha+1,j}^{n+1}} \qquad \alpha = 1...M-1, \qquad (4.5)
$$

$$
c_{\alpha j} = -\frac{2\mu \Delta t^n}{h_{\alpha j}^{n+1} + h_{\alpha-1,j}^{n+1}} \qquad \alpha = 2...M. \qquad (4.6)
$$

We notice that this matrix is a M-matrix i.e. the diagonal terms are strictly positive, the other ones are strictly negative and the diagonal terms are strictly dominant. Therefore the matrix is invertible.

4.3 Properties of the discrete multilayer kinetic scheme

We exhibit in this section that the discrete multilayer kinetic scheme ensures three essential properties of the continuous multilayer model, *i.e.* the positivity of the water height, the preservation of the lake at rest equilibrium and the agreement between the solutions of the monolayer and multilayer Saint-Venant models when there is no friction on the bottom. The proofs are very similar to the classical monolayer case and for the details, we refer the reader to [2].

Theorem 4.1 *Under the CFL condition*

$$
\Delta t \leq \min_j \left(\frac{\Delta x_j}{\max_\alpha \left(|U_{\alpha,j}| + w_\chi \left(\frac{gh_j}{2} \right)^{1/2} \right)} \right), \qquad (4.7)
$$

where w_χ is related to the size of the support of χ, the discrete kinetic multilayer scheme preserves the non negativity of the water height for each layer.

Proof. As the viscous source term takes place in the momentum equation the implicit step does not concern the water heights. Hence it is enough to prove that the finite volume solver preserves the positivity of the water height.

The idea of the proof is then to exhibit that the discrete microscopic density of particle at time $t^{n+\frac{1}{2}}$ is, for all ξ, a convex combination of the Gibbs equilibriums at time t^n and for the neighbouring points. We refer to [2] for the details. The adaptation to the multilayer case is easy. Let us notice that the CFL condition (4.7) is a little more restrictive that the classical monolayer CFL condition - see [2] - since it contains the velocity of the quickest layer. □

Theorem 4.2 *The discrete kinetic multilayer system preserves the stationary states associated to the lake at rest*

$$\forall \alpha = 1...M \qquad \left\{ \begin{array}{l} h_{\alpha j} = h_\alpha, \\ U_{\alpha j} = 0. \end{array} \right. \tag{4.8}$$

Also in the zero friction case with initial data $U^0_{\alpha j} = U^0_j$ and $h^0_{\alpha j} = c_\alpha H^0_j$ (such that $\sum c_\alpha = 1$), the solution of the discrete kinetic multilayer scheme is

$$\forall \alpha = 1...M \qquad \left\{ \begin{array}{l} h^n_{\alpha j} = c_\alpha H^n_j, \\ U^n_{\alpha j} = U^n_j, \end{array} \right.$$

where (U^n_j, H^n_j) is the solution of the classical Saint-Venant kinetic scheme - refer to [2] - with initial data (U^0_j, H^0_j).

Proof. The proof for the preservation of the lake at rest equilibrium is obvious. Nevertheless notice that the discrete lake at rest (4.8) is only a particular case of the continuous lake at rest steady state (3.18). Indeed the continuous lake at rest equilibrium is the result of a balance between two terms while the discrete multilayer scheme preserves this equilibrium only if these two terms vanish separately.

The proof of the second result follows from two facts (i) the source term vanish at each time step for both schemes, (ii) the fluxes of the multilayer scheme are obtained by multiplying the flux of the classical Saint-Venant kinetic scheme by the constants c_α. □

5 Numerical assessment: a dam break problem

We consider the case of a dam break on a flat bottom. This example is used in [15] to compare the classical Saint-Venant system (3.1)-(3.2), the viscous Saint-Venant system (3.3)-(3.4) and the Navier-Stokes equations (2.1)-(2.3). We include in this comparison our new multilayer Saint-Venant model (3.23)-(3.28). We also mention the solution of the homogeneous Saint-Venant system - *i.e.* the classical Saint-Venant system (3.1)-(3.2) with a zero

friction coefficient - since it is very classical in the Saint-Venant litterature.

The main parameters of the computation are the following: viscosity $\mu = 0.01$, gravity $g = 2.0$. The dam is located at the middle of the computational domain. The water is initially at rest and the left and right water heights are respectively equal to two and one meter. We discretize the horizontal domain with two hundred points and we perform the computation with three, six or ten layers in the multilayer Saint-Venant case, ten layers in the Navier-Stokes case. The simulation time is equal to 14 seconds.

5.1 The zero friction case

Firstly we check that in the zero friction case and for convenient initial data the multilayer model coincides with the monolayer Saint-Venant models (classical or viscous) as we announced in the previous Section. The result is obtained with an error of the order of the computer accuracy. On an other hand we can observe in Figure 5.1 that even in the case of a zero friction coefficient and with a constant initial velocity, the horizontal Navier-Stokes velocity is no more constant along the vertical at the end of the computation. This is due to non-hydrostatic effects which we have to keep in mind when we will compare results later.
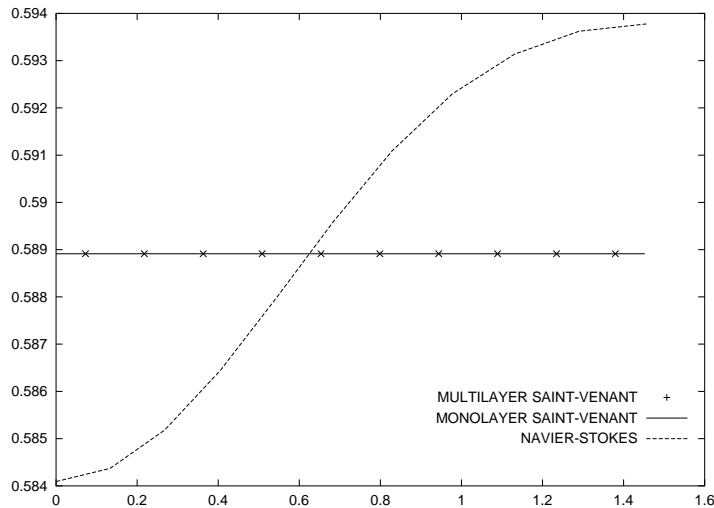
Figure 5.1: VELOCITY (Vertical profiles) - Navier-Stokes and different Saint-Venant models - No Friction - Ten layers

5.2   Comparison with monolayer Saint-Venant models

Second we consider a case with a non zero friction coefficient and we compare the total waterheight - in Figure 5.2 - and the mean velocity - in Figure 5.3 - of the multilayer flow with the waterheight and the velocity of the other Saint-Venant models (homogeneous, classical and viscous).

We first verify that the friction on the bottom has for consequence the decrease of the mean velocity of the flow - since the greatest value corresponds to the homogeneous case. Second it appears that the free surface and velocitiy longitudinal profiles are very different for the classical and for the viscous Saint-Venant systems. Since the viscous system is a more precise approximation of the Navier-Stokes equations it follows that in this case the classical Saint-Venant system fails to correctly characterize the flow. On the other hand the results from the viscous and multilayer Saint-Venant sytems are in very good agreement. It follows that in practice the mean quantities resulting from the multilayer computation are first order approximations of the Navier-Stokes results.
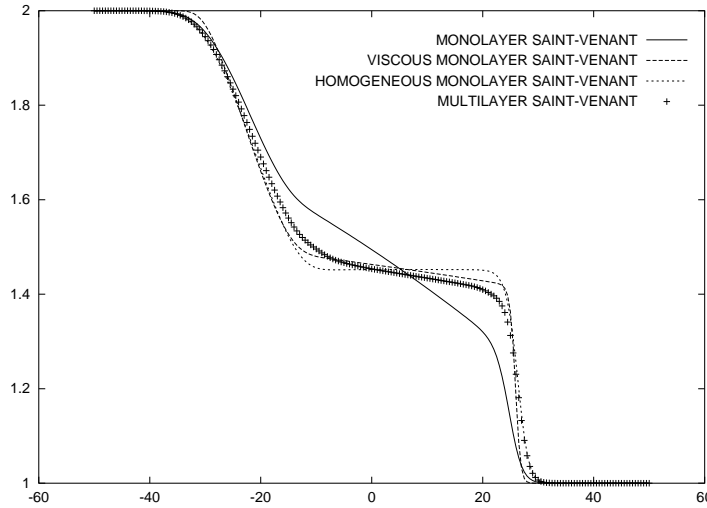
Figure 5.2: FREE SURFACE (Longitudinal profiles) - Different Saint-Venant models - Ten layers - Friction coefficient = .1

5.3   Multilayer aspect of the model

We now investigate the multilayer model by studying the evolution of each layer. We first present the velocity of each layer in Figure 5.4. The results are in accordance with what we could expect: the friction on the bottom makes the lowest layers slower compared to the
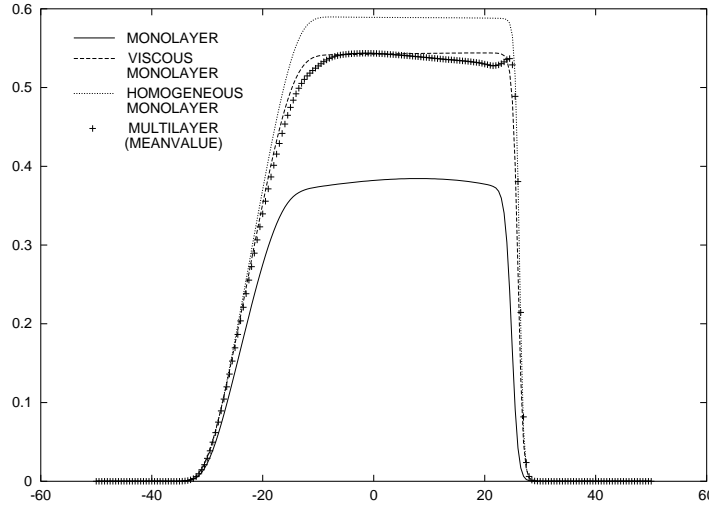
Figure 5.3: VELOCITY (Longitudinal profiles) - Different Saint-Venant models - Ten layers - Friction coefficient = .1

velocity of the viscous Saint-Venant model - and the uppermost layers faster since the mean velocity of the multilayer flow is equal to the velocity of the viscous Saint-Venant model . Notice that the scheme appears to be able to compute large gaps between bottom and free surface velocities. In the case we have considered, the computed velocity for the uppermost layer is four times larger than the velocity computed for the lowest layer. Considering in addition the water heights - Figure 5.5 - it appears also that - except for the lowest layers - the longitudinal profiles of the velocities and the water heights are smooth - even in the neighbourhood of the shock.

5.4   Comparisons with Navier-Stokes velocity profiles

We now compare the two 2D models, *i.e.* the Navier-Stokes equations and the multilayer Saint-Venant system - we recall that we consider in this work only one horizontal direction. First we compare the two computed free surfaces of the flow. In Figure 5.6 we see that the two profiles are very close. In particular the speed of the shock wave and the slope of the free surface between the rarefaction and the shock waves are well computed.

We can now compare the two vertical profiles for the horizontal velocity. The Navier-Stokes profile (along the vertical) is continuous and piecewise linear. The multilayer Saint-Venant profile is constant on each layer and thus discontinuous. We choose to present - for each layer - the velocity at the middle of the layer - considering the vertical component. The multilayer and Navier-Stokes computations are managed with ten layers in the vertical direction. We choose an arbitrary vertical section included in the central zone - $x = 8m$, but what we
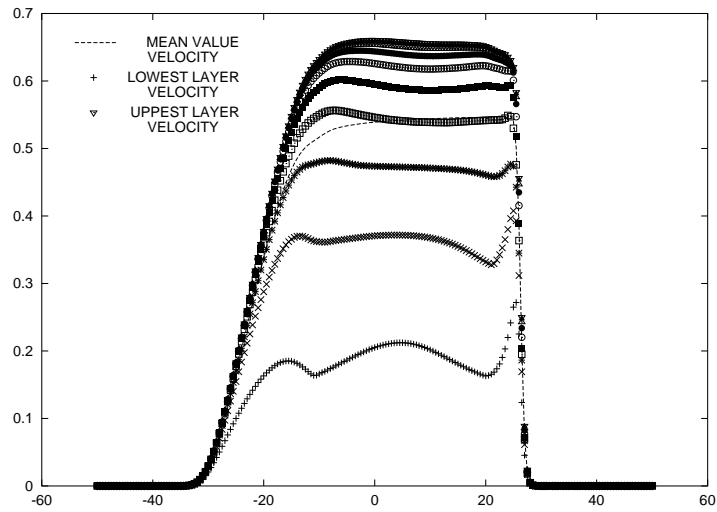
Figure 5.4: LAYER VELOCITIES (Longitudinal profiles) - Mulitlayer Saint-Venant model (each type of cross corresponds to a different layer) - Ten layers - Friction coefficient = .1
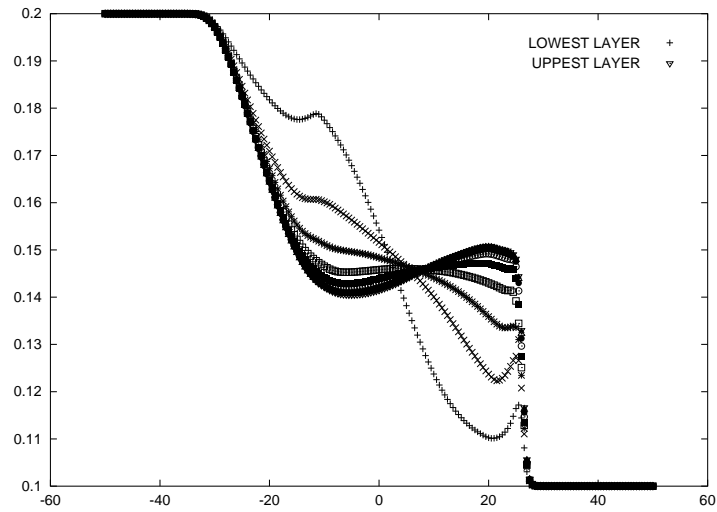

Figure 5.5: LAYER HEIGHTS (Longitudinal profiles) - Multilayer Saint-Venant model (each type of cross corresponds to a different layer) - Ten layers - Friction coefficient = .1

observe is also valid for any section included in this region.

The results are presented in Figure 5.7. The two vertical profiles of the horizontal velocity are in good agreement. In particular notice that both values of the velocity at the bottom and at the free surface are well captured - even though the gap between these two values is large. Between these two extrema the curvature of the multilayer profile seems to be a bit larger than those of the Navier-Stokes profile but the amplitude of this difference is very limited.
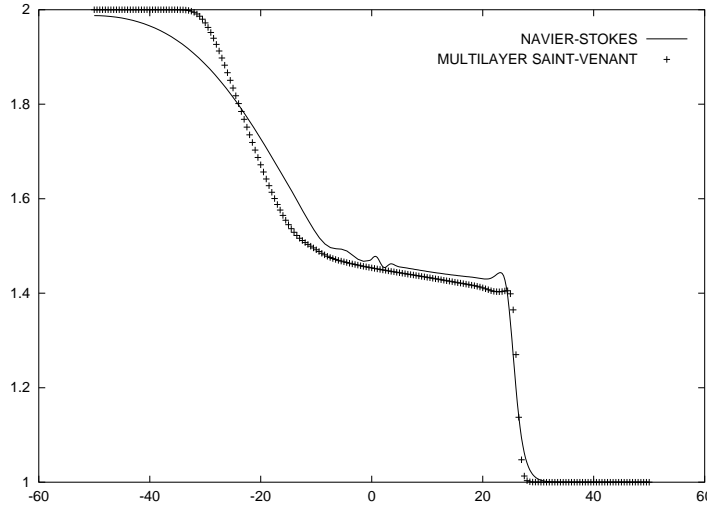
Figure 5.6: FREE SURFACE (Longitudinal profiles) - Navier-Stokes and Multilayer Saint-Venant models - Ten layers - Friction coefficient = .1

5.5   Computational cost

Mono- and multilayer Saint-Venant systems are computed using the same finite volume algorithm. Thus the ratio between their respective computational costs is obviously linked to the number of layers. But the multilayer algorithm implies some supplementary computations - viscous effects. Moreover the multilayer CFL condition (4.7) is linked to the velocity of the fastest layer and thus it is a little more restrictive in the multi- than in the monolayer case. For example, in the considered case, with ten layers, the multilayer computation is about fifteen times more time consuming than the monolayer Saint-Venant one.

The Navier-Stokes algorithm that we used is based on an implicit ALE method with moving meshes. Thus the algebraic computations are much time consuming. Furthermore we consider an instationnary test case. It follows that, for this test case and for the same number of layers, the Navier-Stokes computation is about twenty times more time consuming than the multilayer Saint-Venant one.
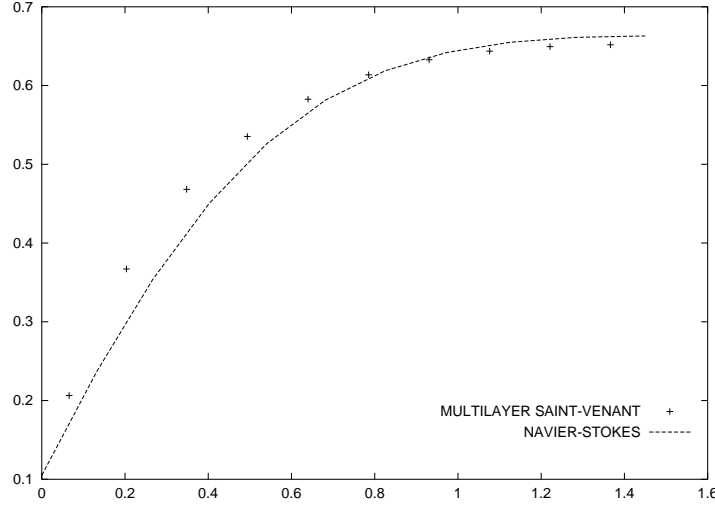
Figure 5.7: VELOCITY (Vertical profiles) - Navier-Stokes and Multilayer Saint-Venant models - Ten layers - Friction coefficient = .1

5.6 Influence of the number of layers

Now we test the influence of the number of layers on the computed multilayer solution. We consider the same test case as before and we compute it with three and six layers. We present in Figure 5.8 the vertical velocity profiles obtained with the Navier-Stokes computation and with the multilayer one for three, six and ten layers. It appears that the multilayer results are in very good accordance with the Navier-Stokes ones as soon as we manage a really multilayer computation, even with a low number of layers. Indeed the computed vertical velocity profile for the three layers case is very close to the Navier-Stokes one. When we increase the number of layers the computed vertical profile seems to tend to a limit profile that is almost but not exactly the Navier-Stokes one - maybe due to the non hydrostatic effects.

5.7 Some other friction coefficients

To end this numerical validation we come back to the ten layers test case but changing the friction coefficient. We present the computed vertical velocity profiles with both Navier-Stokes and multilayer Saint-Venant approaches. In Figure 5.9 we present a small friction coefficient case. The difference between the two profiles is not neglectable and in particular the velocity at the bottom is not very well computed. This phenomenon can be related to the small non hydrostatic deviation that exists for the Navier-Stokes profile in the no friction case - Figure 5.1. Nevertheless let us observe that the difference between the top
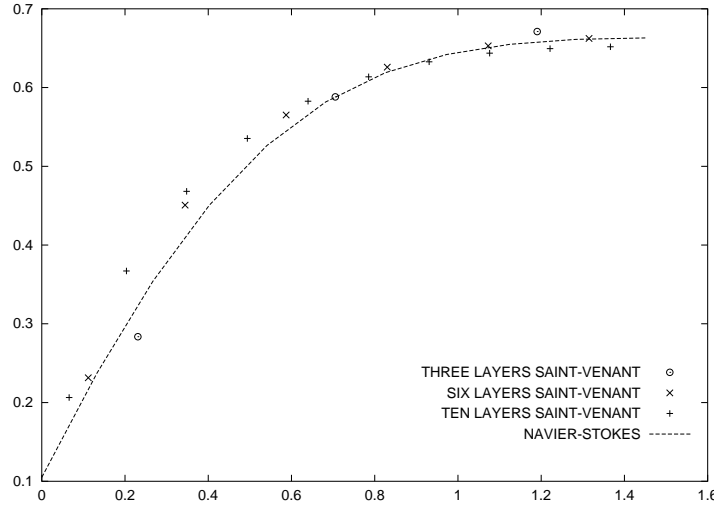
Figure 5.8: VELOCITY (Vertical profiles) - Navier-Stokes and Multilayer Saint-Venant (with different number of layers) models - Friction coefficient = .1

and the bottom velocities does not exceed five per cent and then conclude that this cases are less interesting since for the small coefficients the classical Saint-Venant system is already a good approximation of the Navier-Stokes equations.

In Figure 5.10 we present the no-slip condition case. Notice that for this second example there is no notion of friction coefficient in the Navier-Stokes formalism since we impose that the velocity is equal to zero at the bottom. We extend this boundary condition to the multilayer computation. It follows that the velocity of the lowest layer is equal to zero. Like for the first test case the results are in quite good accordance. This result exhibits the robustness of the model since we are not at all in the asymptotic case from which we deduce the multilayer system since the friction coefficient is infinitely large. It follows that the multilayer Saint-Venant model has a quite large range of validity.

5.8 Robustness of the scheme

We now discuss the robustness of our modified layer-by-layer approach (3.23)-(3.28) when the initial hypothesis of Property (P3) in Proposition 3.4 is violated. The worst case we consider here is when the initial ratio between the water height of one layer and the total water height exhibits a spatial discontinuity.

In [6] such a case occurs. The authors introduce a Q-scheme to study a bi-fluid 1D shallow water system. In particular they compare global upwinding and uncoupled upwinding approachs. If we assume that the densities of the two fluids are equal, the "global upwinding"
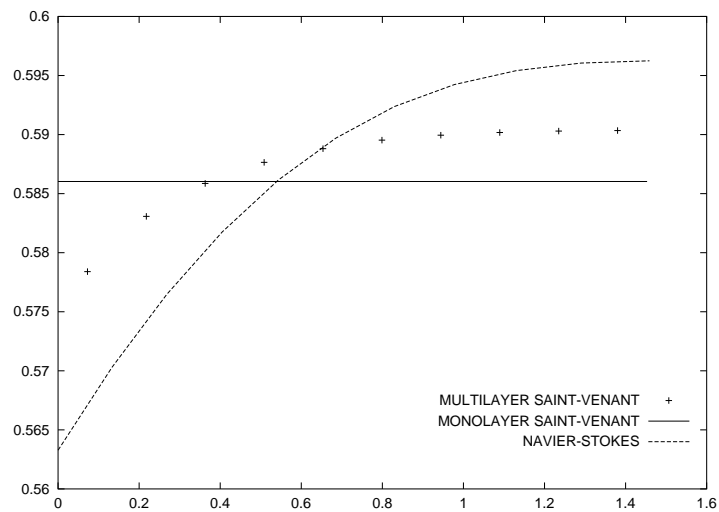
Figure 5.9: VELOCITY (Vertical profiles) - Navier-Stokes and Multilayer Saint-Venant models - Ten layers - Friction coefficient = .001
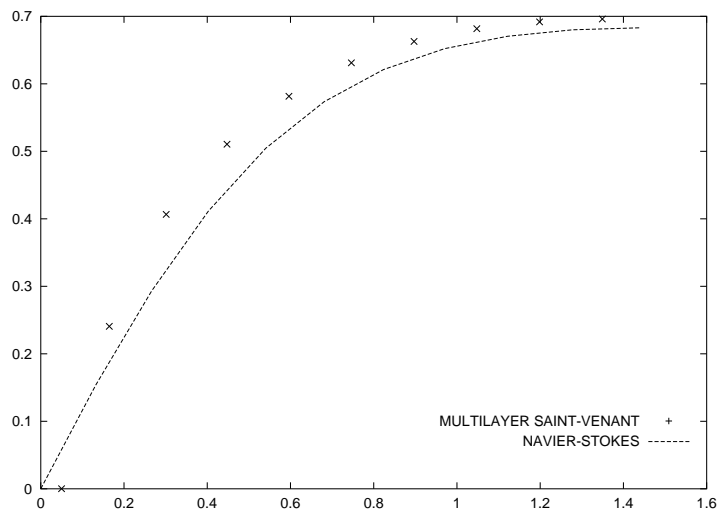

Figure 5.10: VELOCITY (Vertical profiles) - Navier-Stokes and Multilayer Saint-Venant models - Ten layers - No slip

consists in dealing with the 4×4 non conservative system (3.6)-(3.11) whereas the "uncoupled upwinding" corresponds to a basic layer-by-layer approach - see Remark 3.3. A numerical example, that involves a discontinuity in the initial interface, exhibits that the "uncoupled upwinding" strategy leads to large oscillations in the solution - for both interface and free surface.

Here we are interested in studying our numerical method for such a test case. Thus we consider the same initial data (except that in our simulations the two densities are equal) and we do not consider any viscous stabilizing effects (i.e. that viscosity and friction coefficients are equal to zero). Then we compare in Figure 5.11 the results obtained with the basic layer-by-layer approach and with our modified layer-by-layer approach - see Section 4. It appears that our approach allows to avoid such oscillations. In spite of a large number of test cases we have performed, none of them exhibited any numerical instabilities despite the non-hyperbolicity of the system (3.6)-(3.11).
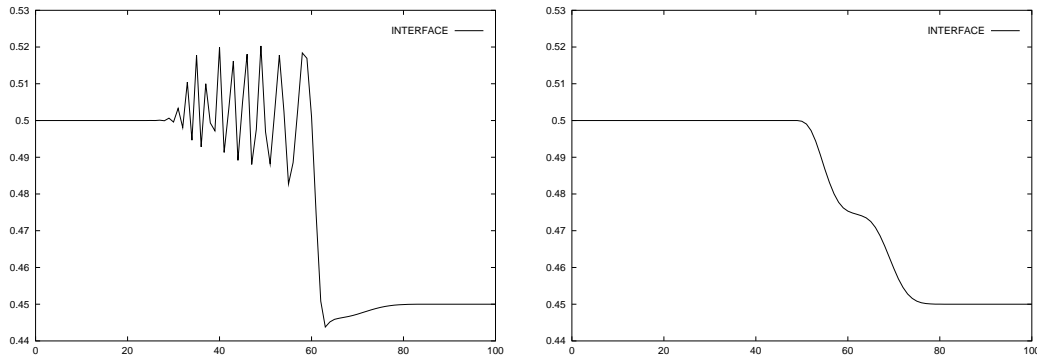
Figure 5.11: Interface profiles for a bilayer test case - The basic (left) and the modified (right) layer-by-layer approachs

6 Conclusion and perspectives

Thanks to a formal asymptotic analysis of the full Navier-Stokes equations for incompressible flows with a free moving boundary under the shallow water assumption, we derive a multilayer Saint-Venant model which allows a non constant vertical profile while preserving the computational efficiency of the classical Saint-Venant model. The model has the same range of validity as the Navier-Stokes hydrostatic model.

This multilayer model verifies some essential stability properties - positivity of the water height, existence of a non increasing energy, hyperbolicity of the conservative part. It ensures also the preservation of some physical requirements as the preservation of steady states or the accordance with the Saint-Venant equation and/or with the Navier-Stokes hydrostatic model for some particular flows.

Numerical comparisons with classical Saint-Venant and full Navier-Stokes computations on a dam break problem validate the model. In particular it appears that the vertical velocity profiles issued from the multilayer Saint-Venant and full Navier-Stokes computations are very close.

Some questions remain open: accordance with the vertical profile of the velocity issued from the Navier-Stokes hydrostatic model - to discriminate the influences of the hydrostatic approximation and of the discretization "à la Saint-Venant", preservation of steady states with topographic terms - this specific problem is well-known to be an essential property of the classical Saint-Venant solvers [1, 3, 18].

Acknowledgements

References

[1] Audusse E., Bouchut F., Bristeau M.O., Klein R. and Perthame B., *A fast and stable well-balanced scheme with hydrostatic reconstruction for shallow water flows*, submitted to SIAM J. Sc. Comp.

[2] Audusse E., Bristeau M.O. and Perthame B., *Kinetic schemes for Saint-Venant equations with source terms on unstructured grids*, INRIA Report, RR-3989 (2000), http://www.inria.fr/RRRT/RR-3989.html

[3] Bermudez A. and Vazquez E., *Upwind methods for hyperbolic conservation laws with source terms*, Comput. Fluids (8) 23 (1994), 1049–1071.

[4] Besson O. and Laydi M.R., *Some estimates for the anisotropic Navier-Stokes equations and for the hydrostatic approximation*, RAIRO M2AN (7) 26 (1992), 855–865.

[5] Bouchut F., Mangeney-Castelnau A., Perthame B., Vilotte J.P., *A new model of Saint-Venant and Savage-Hutter type for gravity driven shallow water flows*, C. R. Math. Acad. Sci. Paris (6) 336 (2003), 531–536.

[6] Castro M., Macias J. and Pares C., *A Q-scheme for a class of systems of coupled conservation laws with source term. Application to a two-layer 1-D shallow water system.* M2AN Math. Model. Numer. Anal. (1) 35 (2001), 107–127.

[7] Castro M.J., Garcia-Rodriguez J.A., Gonzanlez-Vida J.M., Macias J., Pares C. and Vazquez-Cendon E., *Numerical Simulation of two layer shallow water flows through channels with irregular geometry*, submitted to JCP.

[8] Castro M.J. and Pares C. *On the well balanced property of Roe's method for nonconservative hyperbolic systems. Applications to shallow water systems*, preprint.

[9] Causin P., Miglio E., Saleri F., *Algebraic factorizations for 3D non-hydrostatic free surface flows*, Comput. Vis. Sci. (2) 5 (2002), 85–94.

[10] Chacon Rebollo T. and Guillen Gonzalez F. *An intrinsic analysis of existence of solutions for the hydrostatic approximation of Navier-Stokes equations*, C. R. Acad. Sci. Paris, Serie 1, 330 (2000), 841–846.

[11] Dal Maso G., Lefloch P., Murat F., *Definition and weak stability of nonconservative products*, J. Math. Pures Appl. (9) 74 (1995), no. 6, 483–548.

[12] Dafermos C.M., "Hyperbolic conservation laws in continuum physics", Springer Verlag, GM 325 (1999).

[13] Ferrari S., Saleri F., *A new two dimensionnal shallow water model including pressure term and slow varying bottom topography*, to appear in M2AN (2004).

[14] Fontana L., Miglio E., Quarteroni A., Saleri F., *A finite element method for 3D hydro-static water flows*, Comput. Vis. Sci. (2) 2 (1999), 85–93.

[15] Gerbeau J.F. and Perthame B., *Derivation of viscous Saint-Venant system for laminar shallow water ; Numerical validation*, Discrete Cont. Dyn. Syst. Ser. B (1) 1 (2001), 89–102.

[16] Gill A.E., "Atmosphere Ocean Dynamics", International Geophysics Series Vol. 30, Academic Press Inc. (1982).

[17] E. Godlewski, P.-A. Raviart, "Numerical approximation of hyperbolic systems of conservation laws", Applied Mathematical Sciences, 118, Springer-Verlag, New York, 1996.

[18] Greenberg J.M. and LeRoux A.Y., *A well balanced scheme for the numerical processing of source terms in hyperbolic equations*, SIAM J. Numer. Anal. 33 (1996), 1–16.

[19] Guillen Gonzalez F., Masmoudi N. and Bellido R., *Anisotropic estimates and strong solutions of the primitive equations*, Diff. Int. Equ. (11) 14 (2001), 1381–1408.

[20] Hervouet J.M., *A high resolution 2D dam break model using parallelization*, Hydrological Processes (13) 14 (2000), 2221–2230.

[21] Hervouet J.M., Janin J.M., Lepeintre F., Pechon P., *TELEMAC 3D: a finite element software to solve the 3D free surface flow problems*, International Conference on Hydro-science and Engineering, Washington, USA, 1993.

[22] Lazzaroni E., *Approssimazione numerica di modelli multistrato per fluidi a superficia libera* (in italian), Universita degli studi di Milano, Tesi di laurea, 2002.

[23] R.J. LeVeque, "Finite Volume Methods for Hyperbolic Problems", Cambridge University Press, 2002.

[24] Lions P.L., "Mathematical Topics in Fluid Mechanics Vol. 1", Oxford Univ. Press, 1996.

[25] Miglio E., Quarteroni A., Saleri F., *Finite element approximation of quasi-3D shallow water equations*, Comput. Methods Appl. Mech. Engrg. (3-4) 174 (1999), 355–369.

[26] Perthame B., "Kinetic formulations of conservation laws", Oxford Univ. Press, 2002.

[27] Perthame B. and Simeoni C., *A kinetic scheme for the Saint-Venant system with a source term*, Calcolo 38 (2001), 201–231.

[28] de Saint-Venant A.J.C., *Théorie du mouvement non-permanent des eaux, avec application aux crues des rivières et à l'introduction des marées dans leur lit* (in french), C. R. Acad. Sc., Paris 73 (1871), 147–154.

[29] Serre D. , "Systèmes hyperboliques de lois de conservation", Diderot, Paris, 1996.

[30] Whitham G.B., "Linear and non linear waves", John Wiley and Sons Inc., New York, 1999.